PNAS

www.pnas.org

Supplementary Information for

Thermodynamic phase diagram of amyloid-β (16-22) peptides

Yiming Wang[1], Samuel J. Bunce[2,3], Sheena E. Radford[2,4], Andrew J. Wilson[2,3], Stefan Auer [3], Carol K. Hall[1*]

1. Department of Chemical and Biomolecular Engineering, North Carolina State University, Raleigh, NC 27695-7905, United States

2. Astbury Centre for Structural Molecular Biology, University of Leeds, Woodhouse Lane, Leeds LS2 9JT, United Kingdom.

3. School of Chemistry, University of Leeds, Woodhouse Lane, Leeds LS2 9JT, United Kingdom.

4. School of Molecular and Cellular Biology, Faculty of Biological Sciences, University of Leeds, Woodhouse Lane, Leeds LS2 9JT, United Kingdom.

Corresponding Author: Carol K. Hall
 Email: hall@ncsu.edu

This PDF file includes:

> Materials and Methods
> Supplementary text
> Figs. S1 to S8

Materials and Methods

A$\beta_{16\text{-}22}$ solid-phase peptide synthesis (SPPS)

All amino acids and resins were purchased from Novasyn (Merck), Fluorochem or Sigma-Aldrich. All amino acids were *N*-Fmoc protected and the side-chains were protected with Boc (Lys) or OtBu (Glu). A$\beta_{16\text{-}22}$ was synthesized on an automated solid-phase peptide synthesiser (CEM LibertyBlue). (1) DMF used in peptide synthesis was of ACS grade from Sigma-Aldrich. Crude peptide identity was confirmed by LC-MS prior to HPLC purification. A$\beta_{16\text{-}22}$ was purified by preparative scale HPLC using an X-bridge C18 preparative column (reversed phase) on an increasing gradient of MeCN to H_2O ($5 - 95\%$ with 0.1% formic acid) over 15 minutes. The purity of the peptide was confirmed to be above (>95%) by Analytical HPLC and the peptide identity was confirmed by LC-MS. The pure peptide was freeze dried and stored at - 20 °C prior to use.

Aggregation conditions and Transmission Electron Microscopy (TEM)

A$\beta_{16\text{-}22}$ was diluted from a DMSO stock solution (1-30mM) to the required concentration (10-300µM) in 100 mM ammonium bicarbonate buffer (pH=7). Final DMSO concentration was kept at 1% (v/v) in all assays. After a week, aliquots were taken for TEM analysis. If no fibrils were observed, the samples were left to incubate for another week. Conditions under which A$\beta_{16\text{-}22}$ did not form visible fibrils using extensive TEM analysis after two weeks were counted as those under which fibrils do not form. TEM images were taken at the end of each experiment by removing 5 µL and placing the solution on carbon-formvar grids for 30s prior to staining with 2% (w/v) uranyl acetate solution for an additional 30s as described by Preston *et al*.

(2). Images were taken on a JEM-1400 (JEOL Ltd., Tokyo, Japan) transmission electron microscope within the Astbury Biostructure Laboratory.

Supplementary text

Structural difference between the non-HB oligomer and the HB oligomer

We consider the non-HB and HB oligomers to be two distinct states. Although they may look like a continuum of states in Fig. 1, peptides in these two states have different numbers of hydrogen bonds and hydrophobic sidechain contacts with neighboring peptides (see Fig. S1). As shown in Fig. S1A (orange curve) and S1B, peptides in the non-HB oligomer on average have one intra-peptide helical HB formed mainly between Leu17 and Ala21 and sometimes between Val18 and Glu22. The HB oligomer, as shown in Figs. S1A-D, is stabilized by having both a large number of inter-peptide HP contacts (mainly by Leu17, Phe19 and Phe20) and a small number of both inter- and intra-peptide HBs.

System sizes and constraints for measuring solubility for five types of A$\beta_{16\text{-}22}$ aggregates

The small non-HB and HB oligomers contain 7 peptides and the number of monomer peptides in solution is 15. The 2, 3 and 4 β-sheet fibrils contain 24, 28 and 38 peptides, respectively, and the number of monomer peptides in solution is 40. The preformed fibrils are chosen to have around ten peptides in each β-sheet. This system size is large enough for the fibril to shrink, and small enough so that the simulations are feasible, allowing us to determine the concentration at which the fibril neither grows or shrinks based on equilibrium trajectories. (Fig. S7). The initial monomer peptide concentration is chosen to

be relatively high so that the solution phase is supersaturated with respect to equilibrium state. In this way, we prevent the preformed fibrils from fully dissolving into monomers. The choice of a fibril with a different initial length should not affect the equilibrium monomer concentration (solubility) , as was verified in previous work by Auer et al(3). The total computation time for these simulations was 9 months using 25 central processing units (CPU), with each individual run lasting around 50μs to 100μs.

During measurement of the solubility of a non-HB oligomer, all peptides in the system can form intra-peptide hydrogen bonds, but not inter-peptide hydrogen bonds. The latter is accomplished by imposing constraints on the specific collision events that could lead to the formation of such bonds by turning off the attractive square well interactions between the C=O and NH spheres. Similarly, during measurement of the solubility of the HB oligomer, all peptide pairs in the system are constrained to form at most one inter-peptide hydrogen bond. During measurement of the solubility of fibrils with fixed thickness (2, 3, and 4 β-sheets), we start from a high initial peptide concentration to prevent fibrils from losing an existing β-sheet layer. The fibrils are also prevented from creating a new β-sheet layer during the solubility measurement by turning off the attractive square well interactions; in that case the only type of collision between the peptide sidechains spheres within the fibril and those of the peptides in the solution is a hard-sphere collision.
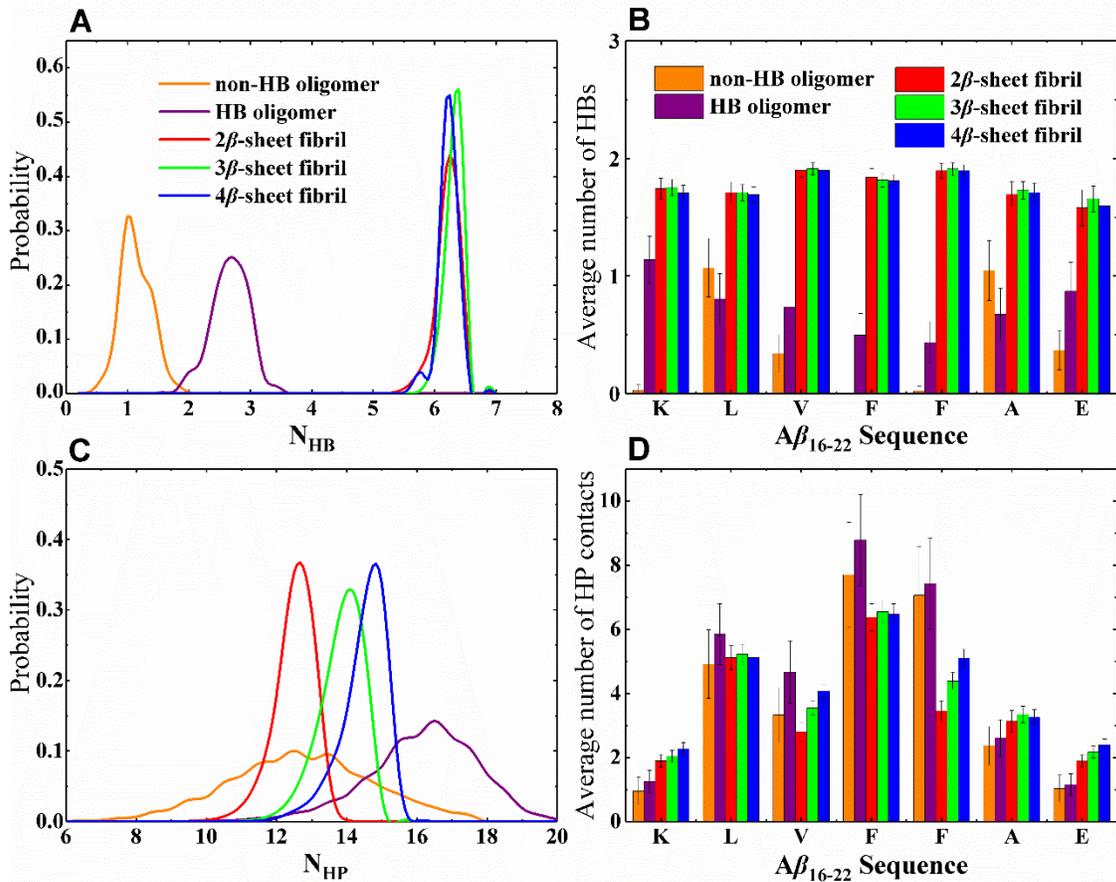
Figure S1. The probability distribution for (A) the average number of hydrogen bonds (N_{HB}) per peptide (counting both intra and inter-molecular HBs) and (B) the average number of hydrogen bonds per residue for the five types of aggregates. The probability distribution (C) for the number of sidechain contacts (N_{HP}) per peptide and (D) the average number of HP sidechain contacts per residue for the five aggregates. The data for the non-HB oligomer (orange) and the HB oligomer (purple) are measured at T=193K and 250K, respectively, and the data for the 2β-sheet (red), 3β-sheet (green) and 4β-sheet (blue) are measured at T=330K. These five aggregates are characterized at different temperatures but similar solubilities, as shown in Fig. 2A.
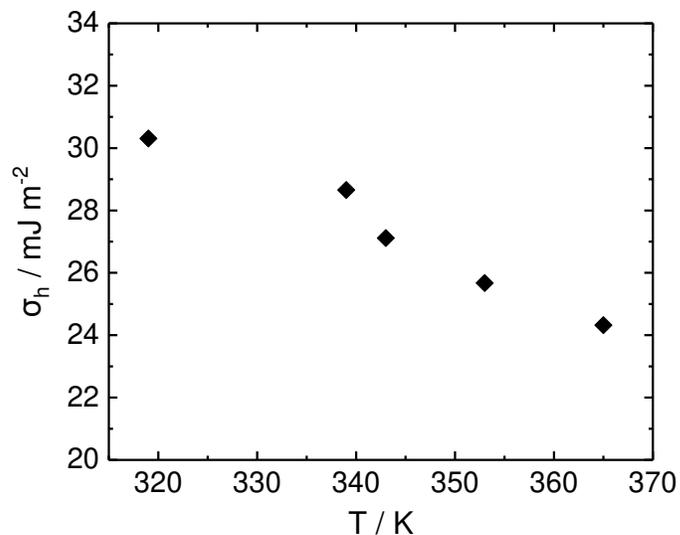
Figure S2. Specific surface energy σ_h (mJ/m^2) of Aβ_{16-22} fibril versus temperature calculated from fitting simulation data ($lnC_{i\beta}$ vs 1/i) to Eq. (2).
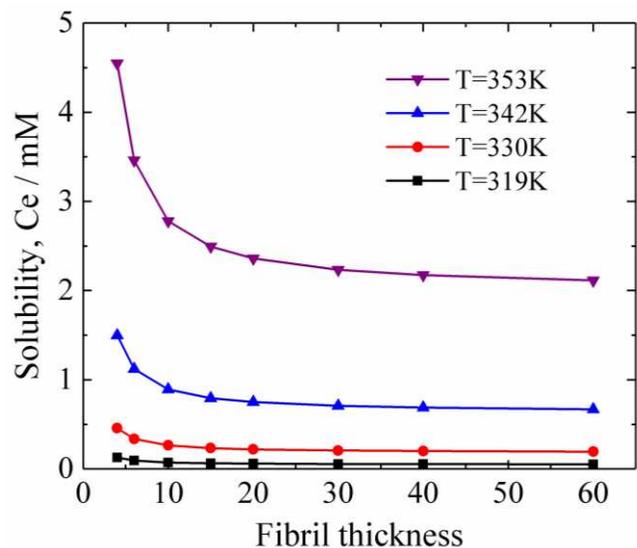
Figure S3. A plot of the estimated solubility of Aβ_{16-22} fibril versus fibril thickness (number of β-sheets) at various given temperatures. Data for this plot are extracted from the linear fit of $lnC_{i\beta}$ - $1/i$ (i=2,3,4) data to Eq. (2) in Fig. 2D.

A $V, T = $ constant

Oligomer phase

Fibril phase

Solution phase

$$\mu_p^{soln(2)}\left(x_p^{soln(2)}\right) = \mu_p^{olig}\left(x_p^{olig}\right)$$

$$\mu_p^{soln(1)}\left(x_p^{soln(1)}\right) = \mu_p^{fib}\left(x_p^{fib}\right)$$

0 $\quad x_p^{soln(1)}\; x_p^{soln(2)} \quad x_p^{olig} \quad x_p^{fib} \quad 1$

x_p
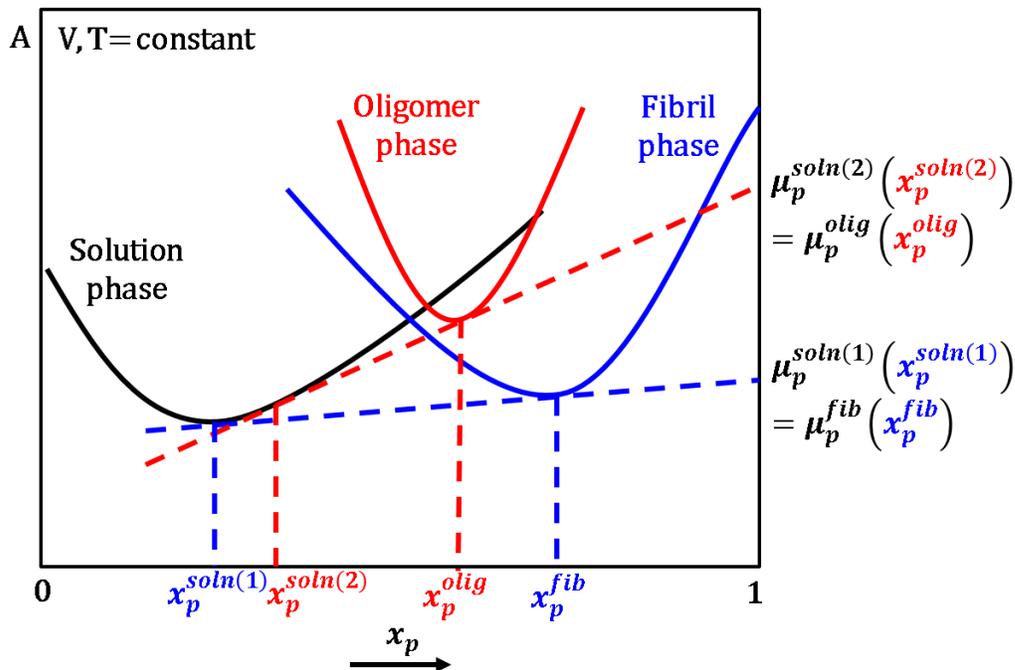
Figure S4. Illustration of the Helmholtz free energy (A) versus peptide composition (x) for a binary (peptide-water) solution system at constant volume (V) and temperature (T). The Helmholtz free energy is considered here instead of the Gibbs free energy because the simulations are done at constant volume rather than constant pressure.

Temperature

Concentration	4 °C	room temp.	37 °C	55 °C
C > 1mM	N.D	✓[4]	✓[5]	✓[6]
200-1000 µM	✓[7]	✓[8]	?	?
100µM	?	?	?	?
50-100µM	?	?	✓[9]	?

Figure S5. Experimental conditions (check marks) under which A$\beta_{16\text{-}22}$ has been shown in literature (4-9) to form fibrillar structures (i.e. at neutral pH). The references used to make this table can be found in the reference list. N.D. means that fibrils are presumed to form but there is no literature study performed under this condition. ? means no experiments have been conducted under these conditions.
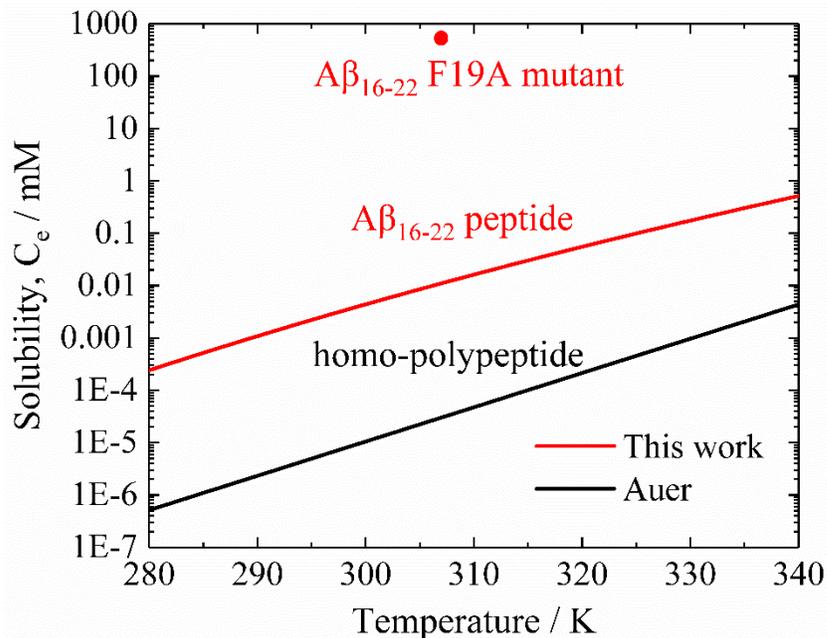
Figure S6. Comparison of the solubility of Aβ(16-22) peptide and its F19A mutant calculated in this work using the PRIME20 model and that of a 12-residue non-sequence-specific peptide calculated by Auer (10).
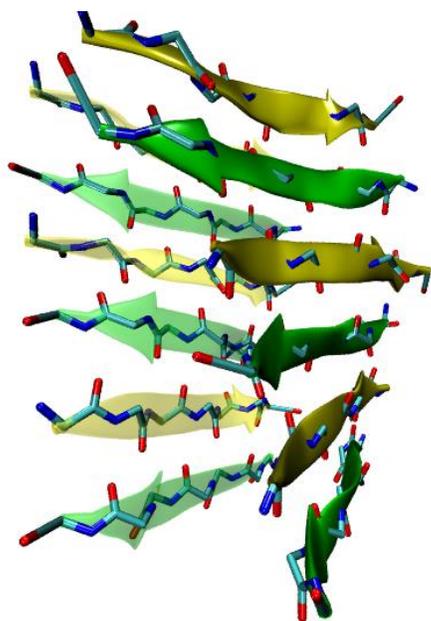
Figure S7. Snaphot from a simulation showing the structure of a two-layer β-sheet fibril of Aβ_{16-22} peptide (colored green and yellow) in an anti-parallel β-sheet configuration. The oxygen (O), nitrogen (NH) and carbon (C$_\alpha$, C=O) groups on the peptide backbone are shown in red, blue and cyan. Note that the sidechain groups are not represented here. The O groups (red) are incorporated into the C=O sphere and do not exist independently in PRIME20 model, the positions of which are determined after simulation.
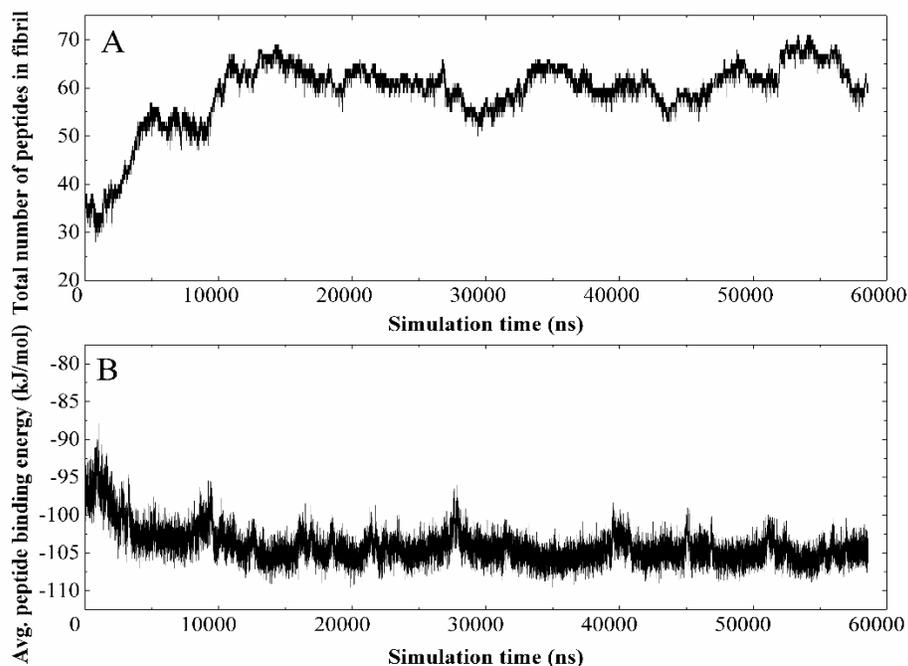
Figure S8. Plots of (A) total number of peptides and (B) the average peptide binding energy (kJ/mol) of a 4β-sheet fibril versus simulation time at T=330K.

References

1. Collins JM, Porter KA, Singh SK, & Vanier GS (2014) High-Efficiency Solid Phase Peptide Synthesis (HE-SPPS). *Org. Lett.* 16(3):940-943.

2. Preston GW, Radford SE, Ashcroft AE, & Wilson AJ (2012) Covalent Cross-Linking within Supramolecular Peptide Structures. *Anal. Chem.* 84(15):6790-6797.

3. Auer S & Kashchiev D (2010) Phase Diagram of alpha-Helical and beta-Sheet Forming Peptides. *Phys. Rev. Lett.* 104(16):168105.

4. Hsieh MC, Liang C, Mehta AK, Lynn DG, Grover MA (2017) Multistep Conformation Selection in Amyloid Assembly. *J. Am. Chem. Soc.* 139: 17007-17010.

5. Childers, WS, Anthony, NR, Mehta, AK, Berland, KM, Lynn, DG (2012) Phase Networks of Cross-β Peptide Assemblies. *Langmuir* 28:6386-6395.

6.   Petty SA, Decatur SM (2005) Experimental evidence for the reorganization of β-strands within aggregates of the Aβ(16-22) peptide. *J. Am. Chem. Soc.* 127:13488-13489.

7.   Preston GW (2012) Analysis of biomolecular interactions using photo-induced covalent cross-linking. PhD thesis, University of Leeds.

8.   Balbach JJ, Ishii Y, Antzutkin ON, Leapman RD, Rizzo NW, Dyda F, Reed J, Tycko R (2000) Amyloid fibril formation by A beta(16-22), a seven-residue fragment of the Alzheimer's beta-amyloid peptide, and structural characterization by solid state NMR. *Biochemistry* 39:13748-13759.

9.   Senguen FT, Lee NR, Gu X, Ryan DM, Doran TM, Anderson EA, Nilsson BL (2011) Probing aromatic, hydrophobic, and steric effects on the self-assembly of an amyloid-β fragment peptide. *Mol. BioSyst.* 7:486-496.

10.   Auer S (2011) Phase diagram of polypeptide chains. *J. Chem. Phys.* 135(17):175103.